

# Dynamic quantized fracture mechanics

N. M. Pugno

Received: 6 May 2005 / Accepted: 7 August 2006  
© Springer Science+Business Media B.V. 2006

**Abstract** A new quantum action-based theory, dynamic quantized fracture mechanics (DQFM), is presented that modifies continuum-based dynamic fracture mechanics (DFM). The crack propagation is assumed as quantized in both space and time. The static limit case corresponds to quantized fracture mechanics (QFM), that we have recently developed to predict the strength of nanostructures. DQFM predicts the well-known forbidden strength and crack speed bands—observed in atomistic simulations—which are unexplained by continuum-based approaches. In contrast to DFM and linear elastic fracture mechanics (LEFM), that are shown to be limiting cases of DQFM and which can treat only large (with respect to the “fracture quantum”) and sharp cracks under moderate loading speed, DQFM has no restrictions on treating defect size and shape, or loading rate. Simple examples are discussed: (i) strengths predicted by DQFM for static loads are compared with experimental and numerical results on carbon nanotubes containing nanoscale defects; (ii) the dynamic fracture initiation toughness predicted by DQFM is compared with experimental results on microsec-

ond range impact failures of 2024-T3 aircraft aluminum alloy. Since LEFM has been successfully applied also at the geophysics size-scale, it is conceivable that DQFM theory can treat objects that span at least 15 orders of magnitude in size.

**Keywords** Dynamic fracture · Quantized fracture · Finite fracture · Nanostructures · Nanotubes · Strength · Impacts

## 1 Introduction

Two classic treatments of linear elastic fracture mechanics (LEFM) are Griffith’s criterion (1920), an energy-based method, and a method based on the stress-intensity factor developed by Westergaard (1939). These have been shown to be equivalent, as in the correlation between (static) energy release rate and stress-intensity factors formulated by Irwin (1957). An extension towards dynamic fracture mechanics (DFM) was proposed by Mott (1948), which included in Griffith’s energy balance the contribution of the kinetic energy. Dynamic stress-intensity factors were then also proposed, as well as the dynamic generalization of Irwin’s correlation, see the Freund’s book (1990). Since LEFM and DFM can be applied only to large and sharp cracks under moderate loading rates, we choose to modify them by accounting for the dis-

---

International Conference on Fracture XI — Symposium 34, on Physics and Scaling in Fracture.

---

N. M. Pugno (✉)  
Department of Structural Engineering, Politecnico di Torino, Corso Duca degli Abruzzi 24, 10129 Torino, Italy  
e-mail: nicola.pugno@polito.it

continuous nature of matter and crack propagation, in both space and time.

Considering a balance of action quanta during crack propagation results in a more flexible theory without ad hoc assumptions. We call this *Dynamics quantized fracture mechanics* (DQFM; note: we use the term “quantized”—as introduced by Novozhilov—not “quantum”, that could be erroneously linked to quantum mechanics). Forbidden strength and crack speed bands clearly emerge. As *quantized fracture mechanics* (QFM; Pugno and Ruoff 2004), allows one to predict the strength of defective structures under quasi-static loading, so DQFM can predict the strength (or the time to failure) under dynamic loading as well as the crack tip evolution. A comparison between QFM and experimental/ numerical investigations on fracture strength of carbon nanotubes (CNTs), and between DQFM and experimental data on the dynamics fracture toughness of 2024-T3 aircraft aluminum alloy, is presented.

A considerable body of literature on fracture in discrete lattices has been developed over the past 25 years. In particular, the earliest work of this kind was probably by Slepian (1981). This was followed by a number of important advances (Marder 1991; Marder and Liu 1993), summarized in a very complete work (Marder and Gross 1995). Moreover, researchers have published a number of related papers (e.g. Pechenik et al. 2002; Heizler and Kessler 2002; Kessler and Levine 2003). Even if all these papers presented important ideas, we believe that our theory still represent an original contribution in this area, as a natural extension of DFM and QFM, in Griffith’s sense. In particular, analytical predictions can be easily obtained by applying DQFM, in contrast to the previously mentioned approaches.

## 2 Dynamic fracture mechanics

According to the principle of conservation of energy, during crack propagation the total energy (sum of the potential  $W$ , kinetic  $T$ , and dissipated  $\Omega$ , energies) is a constant. Thus,  $\partial/\partial A(W+T+\Omega) = 0$ , where  $\partial\Omega/\partial A = G_{dC}$  is the dynamic fracture energy (dissipated per unit area  $A$  created) of the material. The dynamic energy release rate is defined as  $G_d = -\partial(W+T)/\partial A$ . The quasi-static

condition refers to  $T \approx 0$ ; thus, it is simply  $G = G_C$ , with  $G = -\partial W/\partial A$  the (static) energy release rate and  $G_C$  the (static) fracture energy. This represents the well-known Griffith’s criterion, used for predicting the strength of cracked structures under quasi-static external loads. On the other hand,  $G_d = G_{dC}$  allows one to consider dynamic external loads for predicting strength and time to failure and to describe the evolution of the crack tip. Let us assume a crack of length  $l$  and speed  $v = dl/dt$ , where  $t$  is time. From DFM, for a significant family of problems, it is expected that  $G_d(l, t, v) = g(v)G_d(l, t, 0)$ , where  $g(v)$  is a universal function of the crack tip speed (see Freund 1990):

$$g(v) \approx 1 - v/c_R \quad (1)$$

with  $c_R$  Rayleigh’s speed. Introducing the function  $g_C$  as:

$$g_C = \frac{G_{dC}}{G_C} \quad (2)$$

the simplest assumption corresponds to  $g_C \approx 1$ .

The Irwin’s correlation ( $G = (K_I^2/E') + (K_{II}^2/E') + ((1+v)/E)K_{III}^2$ ) connects the (static) stress-intensity factors  $K_{I,II,III}$  for opening (I), sliding (II), and tearing (III) crack propagation modes with the (static) energy release rate  $G$ , through the elastic constants of the material ( $E' = E$  for plane stress, or  $E' = E/(1-v^2)$  for plane strain, where  $E$  is Young’s modulus and  $v$  is the Poisson’s ratio of the material). The extension in the dynamic regime yields the dynamic Irwin’s correlation as  $G_d = (A_I(v)K_{dI}^2/E') + (A_{II}(v)K_{dII}^2/E') + ((1+v)/E)A_{III}(v)K_{dIII}^2$ , where  $K_{dI,II,III}$ , are the dynamic stress-intensity factors and  $A_{I,II,III}(v)$  are universal functions of the crack tip speed  $v$ . In addition, from DFM, for a significant family of problems, it is expected  $K_{dI,II,III}(l, t, v) = k_{I,II,III}(v)K_{dI,II,III}(l, t, 0)$ , where  $K_{I,II,III}(v)$  are again universal functions of the crack tip speed  $v$  (see Freund 1990):

$$\begin{aligned} k_I(v) &\approx \frac{1 - v/c_R}{\sqrt{1 - v/c_D}}, & k_{II}(v) &\approx \frac{1 - v/c_R}{\sqrt{1 - v/c_S}}, \\ k_{III}(v) &\approx 1 - v/c_S, \end{aligned} \quad (3)$$

where  $c_D = \sqrt{\frac{E}{\rho} \frac{1-v}{(1+v)(1-2v)}}$  and  $c_S = \sqrt{\frac{E}{\rho} \frac{1}{2(1+v)}}$  are the longitudinal and shear wave speeds respectively

and  $\rho$  is the material density ( $c_R \approx 0.9c_S$ ). Thus, the dynamic Irwin’s correlation implies in general:

$$A_{I,II,III}(v) = \frac{g(v)}{k_{I,II,III}^2(v)}. \tag{4}$$

By rearranging the previous formulas one derives the condition for the incipient crack propagation in the quasi-static regime ( $T \approx 0$ ) in the stress-intensity factor based treatment, i.e.,  $K_{I,II,III} = K_{I,II,III,C}$ , where  $K_{I,II,III,C}$  are the (static) critical stress-intensity factors or alternatively called the (static) fracture toughness. In dynamics the previous relation becomes  $K_{dI,II,III} = K_{dI,II,III,C}$ , where  $K_{dI,II,III}$  are the dynamic stress-intensity factors and  $K_{dI,II,III,C}$  represent the dynamic critical stress-intensity factors, or the dynamic fracture toughness. Note that to distinguish between  $K_{dI,II,III,C}(v)$  and  $K_{dI,II,III,C}(v = 0)$ , the former is called the dynamic fracture propagation toughness and the latter the dynamic fracture initiation toughness; in the same manner,  $G_{dC}(v)$  and  $G_{dC}(v = 0)$  are the dynamic fracture propagation and initiation energies.

Defining the functions  $k_{dI,II,III,C}$  as:

$$K_{dI,II,III,C} = k_{I,II,III,C}K_{I,II,III,C} \tag{5}$$

for consistency with the energy balance it must be true that:

$$\frac{g_C}{k_{I,II,III,C}^2} = \frac{g(v)}{k_{I,II,III}^2(v)} = A_{I,II,III}(v). \tag{6}$$

We expect  $g_C = g_C(v)$  and  $k_{I,II,III,C} = k_{I,II,III,C}(v)$  and for  $v = 0$   $g_C = k_{I,II,III,C} = 1$ . According to Eq. 6 the dynamic fracture propagation toughness and energy cannot be considered both coincident with their initiation values since  $g_C = k_{I,II,III,C} = 1$  cannot be satisfied for  $v \neq 0$ . In addition, at the incipient crack propagation the dynamic fracture initiation toughness and energy should be identical to their static values. The experiments in general do not agree with this result; however we will show this to be a consequence of adopting the classical criterion rather than due to the real nature of materials.

### 3 Dynamic quantized fracture mechanics

In the DQFM treatment we assume the existence of a fracture quantum and correspondingly the energy balance has to be satisfied during a time

quantum, connected to the time needed to produce a fracture quantum, which is finite as a consequence of the finite crack speed. Thus, the quantization (one might also call it “discretization”) is assumed in both space and time. The energy balance in the continuum space-time is “virtual” and becomes real only for the real formation of a fracture quantum. The classical energy balance is thus rewritten as a quantum action balance, i.e., as:  $\int_{t-\Delta t}^t \Delta(W + T + \Omega)dt = 0$ , where the finite difference is related to the quantized crack advancement; thus, it is equivalent to  $1/\Delta t \int_{t-\Delta t}^t \Delta/\Delta A (W + T + \Omega)dt = 0$ , where  $\Delta A$  and  $\Delta t$  are the time and fracture quanta (the finite variations in the integral are with respect to the crack surface area) and  $1/\Delta t \int_{t-\Delta t}^t \Delta/\Delta A \Omega dt \equiv G_{dC}$ . Thus, DQFM presents an analogy with quantum mechanics as a consequence of the action quantum in each:  $G_{dC} \Delta A \Delta t$ , and  $\hbar$  (Plank’s constant), respectively.

Defining the dynamic quantized energy release rate as:

$$G_d^* \equiv \left\langle (G_d)_A^{A+\Delta A} \right\rangle_{t-\Delta t}^t = -\langle \Delta(W + T)/\Delta A \rangle_{t-\Delta t}^t \tag{7}$$

the criterion  $G_d^* = G_{dC}$  describes the quantized crack propagation under time-dependent loading conditions (here  $\langle f \rangle_{x1}^{x2}$  represents the mean value of  $f$  in the interval  $(x1, x2)$ ).

The quasi-static condition corresponds to QFM and becomes  $G^* = G_C$  (Pugno and Ruoff 2004), where

$$G^* \equiv \langle G \rangle_A^{A+\Delta A} = -\Delta W/\Delta A \tag{8}$$

is the (static) quantized energy release rate (we note that if  $G_d(l, t, v) = g(v)G_d(l, t, 0)$  is valid, then  $G_d^*(l, t, v) = g(v)G_d^*(l, t, 0)$ ). Correspondingly, the dynamic quantized Irwin’s correlation is:

$$G_d^* = \frac{A_I(v)K_{dI}^{*2}}{E'} + \frac{A_{II}(v)K_{dII}^{*2}}{E'} + \frac{1+v}{E}A_{III}(v)K_{dIII}^{*2}, \tag{9}$$

where  $K_{dI,II,III}^*$  are the dynamic quantized stress-intensity factors ( $K_{dI,II,III} > 0$ ) defined by

$$K_{dI,II,III}^* \equiv \sqrt{\left\langle (K_{dI,II,III})_A^{A+\Delta A} \right\rangle_{t-\Delta t}^t}. \tag{10}$$

Thus, the incipient crack propagation in the quasi-static quantized based treatment (Pugno and Ruoff

2004) is  $K_{I,II,III}^* = K_{I,II,III}$ , where

$$K_{I,II,III}^* \equiv \sqrt{(K_{I,II,III}^2)_A^{A+\Delta A}}, \quad (11)$$

whereas in the general dynamic treatment of DQFM it is:

$$G_d^* = G_{dC} \text{ or } K_{dI,II,III}^* = K_{dI,II,III} \text{ (DQFM)}. \quad (12)$$

The criterion  $G_d^* = G_{dC}$  can be used also for mixed mode crack propagation (the crack will propagate in the direction of the maximum energy release rate), whereas the criterion  $K_{dI,II,III}^* = K_{dI,II,III}$  is valid only for pure crack propagation modes.

In contrast to DFM, to apply DQFM for predicting the strength (or time to failure) of solids  $G_{dC} \equiv G_C$  and  $K_{dI,II,III} \equiv K_{I,II,III}$  (for  $v=0$   $g_C = k_{I,II,III} = 1$ ) and thus, an ad hoc dynamic fracture initiation energy or toughness does not have to be postulated.

If  $K_{dI,II,III} = k_{I,II,III}(v)K_{I,II,III}$ , the expressions for  $K_{I,II,III}$  can be derived for hundreds of cases from the stress-intensity factors handbooks (Murakami 1986; Tada et al. 1985). Note that, as the well-known Neuber–Novozhilov (Neuber 1958; Novozhilov 1969) approach, our theory is still based on continuum linear elasticity. There is, in fact, a perfect parallelism between them. Thus, the physical meaning of the stress-intensity factors is obvious. However, we note that the assumption of a discrete crack advancement – intrinsically introducing and quantifying some “nonlinear” effects such as the *R-curve* behaviour – seems to be a powerful tool for treating fracture in also in complex materials.

In our treatment the fracture quantum has to be considered as a characteristic material/structural parameter. At nanoscale it could truly be coincident with the atomic spacing (Pugno and Ruoff 2004), but at larger size-scale it could be, for example, of the order of the grain size or of other macroscopic heterogeneities. In general, it has to be considered as a free parameter to match the result of the tensional approach in the limit of crack length tending to zero. In some cases this corresponds to a fracture quantum increasing with the size-scale and for this reason we have defined it as a material/structural parameter. Similar considerations hold for the time quantum. However, we

believe that the physics behind the fracture and time quanta is connected to the discrete nature of the energy flux during the crack propagation.

Equations (1–12) define DQFM completely, predicting the failure strength  $\sigma_f$ , the time to failure  $t_f$  and the dynamic crack tip evolution  $v(t)$ , for general time-dependent loading conditions  $\sigma = \sigma(t)$ , assuming the energy release rate to be quantized in both space and time. DQFM treats any defect size and shape (as QFM, see Pugno and Ruoff 2004) and loading rate. It is evident that interesting limit conditions for DQFM are (we now omit the symbols I,II,III):

$$\begin{cases} DQFM : G_d^* = G_{dC} \equiv g_C G_C, K_d^* = K_{dC} \equiv k_C K_C \\ \Delta t = 0, v = 0 \rightarrow QFM : G^* = G_C, K^* = K_C \\ \Delta A = 0, \Delta t = 0 \rightarrow DFM : G_d = G_{dC}, K_d = K_{dC} \\ \Delta A = 0, \Delta t = 0, v = 0 \rightarrow LEFM : G = G_C, K = K_C \end{cases}$$

#### 4 The tensional analog of the action-based DQFM

Let us assume a fracture quantum of length  $a$  (e.g.,  $\Delta A \equiv ah$  in a plate having height  $h$ ). The time quantum is expected to be of the order of  $\Delta t \approx a/v$ . Indicating with  $\sigma_y$  the stress acting at the tip (placed at  $x = 0$ ) of a defect, the stress analog of DQFM for the strength prediction must be written as:

$$\sigma_d^* \equiv \frac{1}{a\Delta t} \int_{t-\Delta t}^t \int_0^a \sigma_y(x, t) dx dt = \sigma_C. \quad (13)$$

This crack propagation criterion has been formulated as the dynamic extension of the Neuber–Novozhilov criterion (Neuber 1958; Novozhilov 1969) and successfully applied in the study of dynamic crack propagation under high loading rate conditions by Morozov et al. (1990; see also Petrov 1996) that consider  $\Delta t$  as an incubation time to failure, a characteristic relaxation time upon microfracture of a material. The analogy with DQFM for predicting the structural strength and time to failure for pure crack modes is evident by rewriting the DQFM criterion for crack propagation as:

$$K_d^* = \sqrt{\frac{1}{a\Delta t} \int_{t-\Delta t}^t \int_a^{l+a} K_d^2(x, t) dx dt} = K_C. \quad (14)$$

where  $l$  denotes the crack length.

### 5 The equation of the dynamic $R$ -curve and of the dynamic fracture resistance

For the continuum approach, the measured (super-script (m)) dynamic fracture energy (which is undefined in the classical treatment)  $G_{dC}^m$  is a function (the so-called  $R$ -curve) of geometry, length and crack/loading speed (and it is thus not a material property, see Hellan 1985). To obtain the same predictions of DQFM by applying the classical DFM, one is forced to assume an unrealistic dynamic resistance curve (thus not a material property, e.g., a function of the crack length, structural size and shape, time to failure, and so on. . .)  $G_{dC} \rightarrow G_{dC}^{(m)} \equiv R$ . By comparing the DQFM and DFM treatments, we find:

$$R = g_C G_C + G_d - G_d^* \tag{15}$$

Accordingly, if the continuum approach is used in the stress-intensity factor treatment, one would measure (subscript (m)) a dynamic fracture toughness:

$$K_{dC}^{(m)} = k_C K_C + K_d - K_d^* \tag{16}$$

observed to be different from  $K_C$  (or equivalently  $R$  from  $G_C$ , also at the incipient crack propagation (where  $v=0$  and  $g_C = k_C = 1$ ) (see Hellan 1985). In contrast to DQFM, continuum approaches are unable to explain why at the incipient crack propagation  $R$  is different from  $G_C$ , or  $K_{dC}^{(m)}$  from  $K_C$ . As we are going to show, DQFM is able to quantitatively predict such a fictitious discrepancy.

### 6 Simple examples of applications strength, time to failure, and crack tip equation

We consider the Griffith's case (a) of a linear elastic infinite plate in tension, of uniform thickness  $h$ , with a crack initial length  $2l_0$  orthogonal to the applied far field (crack opening Mode I). The material is described by the fracture toughness  $K_{IC}$  and the fracture quantum at the considered size-scale  $\Delta A \equiv ah$ . For this case, as it is well known,  $K_I(l) = \sigma \sqrt{\pi l}$ , where  $\sigma$  is the applied time-independent far field stress. In this first simple case we thus consider a time independent stress-intensity factor. Accord-

ing to DQFM (or QFM) the failure strength is:

$$\sigma_f = \frac{K_{IC}}{\sqrt{\pi(l_0 + a/2)}} \tag{17}$$

Note that in this case the tensional analog (the static case of Eq. 13 and developed by Neuber-Novozhilov (Neuber 1958; Novozhilov 1969), considering the complete stress field at the tip of a crack, gives the *identical* result but in a less simple way, as demonstrated in (Taylor et al. 2005) in which basically an extensive data fitting of QFM to larger size experiments is successfully presented. Inverting Eq. 17, the fracture quantum can be estimated from the mechanical properties at a given size-scale,  $\sigma_C = \sigma_f(l_0/a \rightarrow 0)$  and  $K_{IC}$ , as  $a = 2K_{IC}^2/(\pi\sigma_C^2)$ .

Let us assume in this example for the sake of simplicity  $g_C \approx 1$  and  $G_d \approx g(v)G$ . The dynamic evolution under the constant applied stress  $\sigma_f$  causing the initiation of the crack propagation, is predicted by DQFM as:

$$\frac{v}{c_R} = 1 - \frac{l_0 + a/2}{l + a/2} \tag{18}$$

According to Eq. 18 the Griffith's crack is predicted to be unstable. The time evolution of the crack tip could be obtained by solving the differential equation (18), where  $v = dl/dt$ . For LEFM and DFM, the predictions of Eqs. 17 and 18 would be the same if the fracture quantum is assumed to be negligible. As expected, the results of the quantized approach tend to the classical values if the continuum hypothesis  $a/l, a/l_0 \rightarrow 0$  is made. The corresponding result for  $\sigma_f$ , in contrast to Eq. 17, would be without meaning for  $l_0 \rightarrow 0$ , predicting an infinite ideal strength. In contrast, if the fracture quantum corresponds to the atomic size, the ideal strength  $\sigma_C = \sigma_f(l_0/a \rightarrow 0)$  predicted by Eq. 17 is identical to Orowan's prediction (1948) if multiplied by a factor of  $\sqrt{\pi/4} \approx 1$ , as discussed also by Pugno and Ruoff (2004). Note that the experimentally observed asymptote of  $v/c_R < 1$  for  $l/l_0 \rightarrow \infty$  can be explained by generation of secondary cracks from the tip of the predominant one (Holland and Marder 1999) and thus can not be deduced from the pure Griffith's case (i.e., Eq. 18), in which no interacting cracks are considered.

By applying Eq. 15, and assuming  $v = 0$ , we find the expression of the (static)  $R$ -curve as:

$$R = \frac{G_C}{1 + a/(2l_0)}. \quad (19)$$

thus, as expected (see Hellan 1985),  $R$  increases and tends to  $G_C$  for crack length tending to infinity.

Taking into account the blunting of the crack tip (for example, due to the opening of two dislocations at the tip, see Holland and Marder 1999), we have to make the substitution  $G_C \rightarrow G_C(1 + \rho_0/2a)$  in the previous equations (Pugno and Ruoff 2004). Equations 17 and 18 would become:

$$\sigma_f = K_{IC} \sqrt{\frac{1 + \rho_0/2a}{\pi(l_0 + a/2)}} = \sigma_C \sqrt{\frac{1 + \rho_0/2a}{1 + 2l_0/a}}, \quad (20)$$

$$\frac{v}{c_R} = 1 - \frac{l_0 + a/2}{l + a/2} \frac{1 + \rho/2a}{1 + \rho_0/2a}, \quad (21)$$

where  $\rho$  and  $\rho_0$  are the tip radii of the cracks of length  $l$  and  $l_0$  respectively, and  $\sigma_C = \sigma_f(l_0 = 0, \rho_0 = 0)$ . Note that, if the continuum hypothesis is made ( $a/l_0, a/\rho_0 \rightarrow 0$ ), Eq. 20 yields practically the same result as the classical tensional approach (maximum stress equal to material strength), for which the stress concentration ( $\sigma_C/\sigma_f$  is  $1 + 2\sqrt{l_0/\rho_0} \approx 2\sqrt{l_0/\rho_0}$  (small radii) as given by the Theory of Elasticity. Thus, Eq. 20 represents the link between concentration and intensification factors. It predicts a finite strength that is size-dependent (in contrast with the continuum tensional approach coupled with the Theory of Elasticity) for geometrical self-similar defects in an infinite plate.

We consider a complementary case (b), a stationary crack, for which the stress-intensity factor is independent from the crack length. In particular, a semi-infinite crack in an otherwise unbounded body is considered. The body is initially stress free and at rest. At time  $t = 0$  a self-balanced antiplane shear  $\tau$  begins to act on the crack faces. In this case, as it is well known,  $K_{III}(t) = 2\tau\sqrt{\frac{2cs t}{\pi}}$  (see Freund 1990). The time to failure  $t_f$  is predicted by DQFM to satisfy the following relationship ( $t_f > \Delta t$ ):

$$2\tau\sqrt{\frac{2cs}{\pi}} = \frac{K_{IIIc}}{\sqrt{t_f - \Delta t/2}}. \quad (22)$$

Note that, according to our time quantization, a minimum time to failure exists and it must be of

the order of  $t_{f \min} \approx \Delta t$ . This could represent an additional physical meaning of the time quantum. On the other hand, by applying DFM, we obtain the same result of Eq. 22 if the time quantum is neglected. The equation of the  $R$ -curve, according to Eq. 15, for  $v = 0$  is:

$$R = \frac{G_C}{1 - \Delta t/(2t_f)}, \quad (23)$$

and it decreases, tending to  $G_C$  when time to failure tends to infinity. Since  $t_{f \min} \approx \Delta t$ , for this case, the measured dynamic fracture initiation energy is predicted approximately to be twice its static value by varying the time to failure within several orders of magnitude. If one applies the classical DFM, then, according to DQFM, an “apparent” dynamic resistance, doubled with respect to the static value, is obtained. This behaviour is observed experimentally, as we will discuss in the following.

## 7 Strength and crack speed forbidden bands

Let us reconsider the Griffith’s case. As stated for DQFM the crack length is quantized, and so  $2l_0 = n_0 a$  and  $2l = na$ , ( $n_0$  and  $n$  are non negative integer numbers) from which the quantization of the strength and crack speed can be deduced. For the Griffith’s case, from Eqs. 20 and 21 and assuming a blunt crack due to adjacent vacancies (i.e.,  $2\rho \approx a$ ), and time-independent blunt tips ( $\rho_0 \approx \rho$ ) we have:

$$\sigma_f = \sigma_C \sqrt{\frac{5/4}{1 + n_0}}, \quad n_0 > 0, \quad (24)$$

$$\frac{v}{c_R} = 1 - \frac{1 + n_0}{1 + n}, \quad n \geq n_0 \geq 0. \quad (25)$$

The first (and largest) forbidden strength band (between  $\sigma_C$  and the prediction for  $n_0 = 1$ ) is in the range  $(1 - 0.8)\sigma_C$ ; atomistic simulations of two-dimensional lattices with adjacent vacancies quantitatively agree with such forbidden bands (see Pugno and Ruoff 2004); for example just one vacancy is expected to reduce the strength by a factor of  $\sim 20\%$ . Furthermore, DQFM derives forbidden crack speed bands. Starting from our simple assumption of  $g_C = 1$ ,  $G_d = g(v)G$ , the first band (between the predictions for  $n = n_0, n_0 + 1$ ) is in the range  $(0 - (1 + n_0)/(2 + n_0))v/c_R$ ; the smallest ( $n_0 = 0$ ), corresponding to the crack initiation

from a plain specimen, is  $(0 - 0.5)v/c_R$ . Atomistic simulations of crack evolution in two-dimensional lattices qualitatively show such forbidden bands (see Holland and Marder 1999). They imply hysteretic crack motion (hysteretic cycles in the crack speed versus applied load curves), known as “lattice trapping”. Postulated since the early 1970s, it has been observed numerically but never experimentally (see Holland and Marder 1999). Due to the large size scale of the experiments (implying large preexisting cracks, i.e., large values of  $n_0$ ) such strength and crack speed forbidden bands are difficult to observe; on the other hand, in contrast to continuum based theories, DQFM implies such strength and crack speed “quantizations”, which may be detectable in nanoscale experiments.

### 8 Static resistance: an application for predicting the fracture strength of defective nanotubes

The strength and fracture of the outer shell of multi-walled (MW) carbon nanotubes (CNT<sub>s</sub>) is reported by Yu et al. (2000). The tensile strengths of this outer shell for 19 individual MWCNTs were measured with a *nanostressing stage* having two opposing atomic force microscope (AFM) tips, and operated in a scanning electron microscope (SEM). This tensile strength ranged from 11 to 63 GPa for the set of 19 MWCNTs that were loaded (in particular, values of 63, 43, 39, 37, 37, 35, 34, 28, 26, 24, 24, 21, 20, 20, 19, 18, 18, 12, 11 GPa were measured).

From such experimental results, distinct clusters of a series of decreasing values of strength, with the maximum 63 GPa, and other values at 43, and in the ranges 36–37, 25–26, 19–20 and 11–12 GPa, were observed. The highest measured value of 63 GPa is lower than the ideal tensile strength of small diameter CNTs, recently obtained with *ab-initio* density functional theory (DFT, Ogata and Shibutani 2003). If the fracture quantum is assumed to be the distance between two adjacent broken chemical bonds, i.e.,  $a \approx \sqrt{3}r_0$ , with  $r_0 \approx 1.42 \text{ \AA}$  and adjacent vacancies are considered, i.e.,  $2l_0 = n_0a$  in Eq. 20, the predicted strength quantizations for  $n_0 = 2, 4, 6, 8$  (with  $\rho_0 \approx 0.8a \approx 2.0 \text{ \AA}$ , shown in Fig. 1a) are in close agreement with molecu-

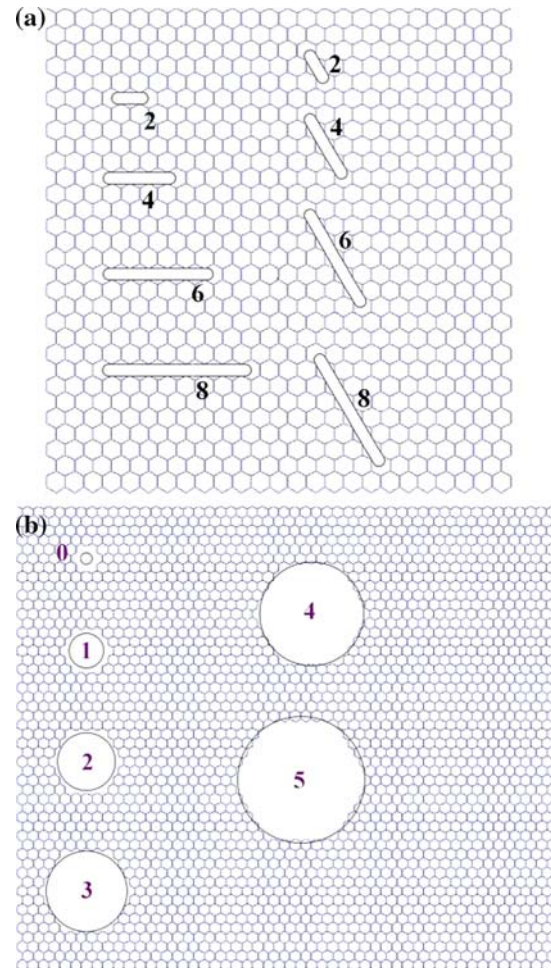


**Fig. 1** (a) Atomic  $n$ -vacancy defects and short blunt cracks used for predicting the strength with QFM (Pugno and Ruoff 2004): the crack length was imposed as  $na$ , whereas the blunt tip radius was chosen to fit the ideal nanotube strength; as shown, the blunt tip radius appears to be reasonable. The fracture quantum length  $a$  is the distance between two adjacent parallel C–C bonds. (b) Holes used for predicting the strength with QFM (Pugno and Ruoff 2004). The fracture quantum is again fixed as identical to the length between two adjacent parallel C–C bonds. (Note that “opened bonds” are not shown in the figure, and for this reason it appears as if the smallest circles seem to “underestimate” the defect size (in reality, they do not))

lar mechanics (MM) calculations (Belytschko et al. 2002), see Pugno and Ruoff (2004). The result is that the strength is strongly reduced by the presence of the nanoflaws. Thus, that *materials become insensitive to flaws at nanoscale* (Gao et al. 2003) cannot be considered of general validity.

The initial crack speed, for the different cases of  $n_0 = 2, 4, 6, 8$ , would be estimated to be respectively of  $v/c_R = 3/4, 5/6, 7/8, 9/10$  (but we note that such estimations refer to the overly simplified assumption of  $g_C = 1, G_d = g(v)G$ ).

Different kinds of defects, such as holes, might be more stable than crack-like defects at the nanoscale (Hirai et al. 2003; Mielke et al. 2004). Nanotubes with “pinhole” defects have been recently investigated by molecular dynamics (MD) simulations (Hirai et al. 2003). In this context, quantum mechanical calculations using DFT semi-empirical methods and MM simulations have been recently performed (Mielke et al. 2004). The results of the atomistic simulations were compared with QFM, with close agreement (nano-holes are as shown in Fig. 1b). We assumed for such (large) nanotubes as the outer shell in the 19 MWCNTs (the diameter varied from 20 nm to 40 nm), that the cross-section reduction due to the presence of defects was negligible. Interestingly, enforcing this constraint the strength tends asymptotically to a finite value (1/3.36 of the strength of the structure without the hole according to QFM, in agreement with MM simulations, see Pugno and Ruoff 2004); this is however still larger than the smallest values experimentally measured. Perhaps (i) sharper defects as discussed above, or (ii) larger holes (breakdown of the assumption of no reduction in cross-section), or (iii) “small” holes satisfying the cross-section constraint, but close and thus causing a greater stress concentration between them than would be the case if they were isolated, are all possible reasons for strength values as low as 11 GPa.

An additional intermediate type of defect was numerically treated by Zhang et al. (2004); corresponding to an elliptical hole with size that we define by an index  $i$ . Starting from a hole obtained removing 6 atoms at the vertexes of an hexagon ( $i = 1$ ) the other defects, corresponding to larger sizes and indexes  $i$ , are obtained removing the lateral four carbon atoms at each blunt tip (see Table 1). The comparison between QFM (only the case of pinhole defect  $i = 1$  was treated by Pugno and Ruoff 2004, whereas here we simply consider  $\rho_0 \approx 0.9a$  and  $l \approx (2i - 1)r_0$ ,  $i = 2, 3, 4, 5$ , in Eq. 20) and atomistic simulations (Zhang et al. 2004) is reported in Table 1. However, we note

that the numerically observed strength asymptote for increasing crack length is “unexpected” and thus unclear, in fact for such a case the crack becomes macroscopic and classical fracture mechanics would suggest the strength decreasing to zero.

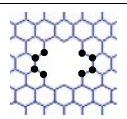
Considering an ideal strength for the experimentally investigated MWCNTs of 93.5 GPa (as computed by Belytschko et al. 2002), the corresponding strength for an  $i = 1$  defect is 64 GPa (compared to the measured value of 63 GPa), for an  $i = 3$  defect is 43 GPa (in agreement with the measured value), for an  $i = 4$  defect is 37 GPa (against the measured value of 39 GPa), for  $i = 5$  defect is 34 GPa (against the measured values of 35 and 34 GPa), for  $i = 6$  defect is 30 GPa (against the measured values of 28 GPa), and so on. This could represent a more plausible scenario (since elliptical holes are chemically more stable than crack-like defects) compared to the assumed linear defects (and circular holes) that were discussed by Pugno and Ruoff (2004). LEFM cannot treat blunt, or short cracks, or holes; DQFM/QFM can.

## 9 Dynamic resistance: an application for predicting the time to failure under impacts

In this section we refer to the experimental work discussed by Owen et al. (1998) on 2024-T3 aircraft aluminium alloy impacts. Petrov and Sitnikova (2004) applied Eq. 13 with respect to time considering only the asymptotic part of the stress field, thus  $\sigma_y(t) \propto K_I(t)$  (and  $\sigma_C \propto K_{IC}$ ), to rationalize some of the experimental results by Owen et al. (1998). The expression of the dynamic stress-intensity factor as applied to the experiments is obtained by considering an infinite elastic plane containing a semi-infinite crack subjected at  $t = 0$  to a linearly increasing impact load. The measured dynamic fracture initiation toughness can be obtained according to Eqs. 14 and 16, where here  $v = 0$ , so that  $k_C = 1$ . According to DQFM, we find the result:  $K_{dIC}^{(m)}/K_{IC} = 2t_f^{3/2} \sqrt{\Delta t} / \sqrt{t_f^4 - (t_f - \Delta t)^4}$ , thus as a function of the time to failure. This function is reported as the solid line in Fig. 2 assuming  $\Delta t = 50 \mu\text{s}$ , whereas the dots refer to the DFQM tensional analog of Eq. 13 fitted with good agreement with the experimental results assuming  $\Delta t = 40 \mu\text{s}$ . Since the two criteria are different,



**Table 1** Comparison between fracture strengths of a (50,0) carbon nanotube, obtained by MM and by QFM, with elliptical holes of size  $i$  (the graph shows the example of  $i = 1$  and the atoms (in black) that would be removed to generate the  $i = 2$  defect)

$\sigma/\sigma_c$	$i=1$	$i=2$	$i=3$	$i=4$	$i=5$	$i=6$	
Theo.	0.68	0.57	0.46	0.40	0.36	0.32	
Num. (50,0)	0.64	0.51	0.44	0.40	0.37	0.34	

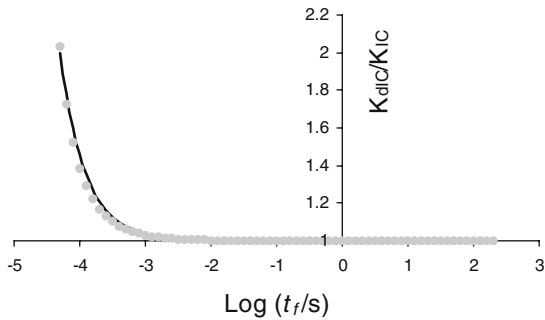


**Fig. 2** Dynamic fracture initiation toughness over (static) fracture toughness, as a function of time to failure for 2024-T3 aircraft aluminum alloy. Solid-line obtained by DQFM ( $\Delta t = 50\mu s$ ); the dots are from the tensional analog of DQFM shown to be in good agreement with the experiments when fitted using  $\Delta t = 40\mu s$  (see Petrov and Sitnikova 2004)

different values for  $\Delta t$  were expected; however we note that the two values are close. In addition, we note that from the DQFM prediction, a minimum time to failure  $t_f \approx \Delta t$  is expected, corresponding to a dynamic fracture initiation toughness of  $K_{dIC}^{(m)} \approx 2K_{IC}$ . Note that Owen et al. (1998) report the observation of “a minimum time necessary to initiate crack growth”, of the order of  $t_f \approx 75\mu s$ , and a dynamic fracture initiation toughness that “reveals an increase of a factor of  $\sim 2$ , as the loading rate increases by seven orders of magnitude” (or as the time to failure decreases). DQFM is thus in good agreement with the experimental data and with the criterion of Eq. 13.

DFM is unable to explain such observations (e.g., the apparent variation of the dynamic fracture initiation toughness). DQFM offers explana-

tions and it is of interest to see further experimental data with which it could be assessed.

### 10 Concluding remarks

DQFM has been presented and used to study the strength and time to failure of solids, as well as the time evolution of the crack tip, also at nanoscale.

For example DQFM can be used as a tool in the design of the *Space Elevator* megacable based on CNTs (since no experiments or numerical atomistic simulations could be used for such a large scale). For example, assuming in such a cable large holes (very likely as a consequence of its large size Carpinteri and Pungo 2005), DQFM predicts an asymptotic limit value of  $\sigma_c/\sigma_f = 3.36$ ; thus, assuming the ideal nanotube strength of  $\sigma_c = 93.5\text{GPa}$  (Belytschko et al 2002), we obtain a failure stress of 28 GPa. Considering in addition the actual nanotube cross-section area, we estimate the ratio between the resistant and apparent cross-section area as  $\eta \approx \pi(R_e^2 - R_i^2)/(2\sqrt{3}(R_e + d/2)^2)$ , with  $R_i, R_e$  the inner and outer nanotube radii and  $d \approx 0.334\text{nm}$  (i.e., the interlayer carbon spacing); for  $R_i \approx 0$  and  $R_e \gg d$ ,  $\eta \approx \pi/(2\sqrt{3}) \approx 0.9$  and the prediction for the cable strength is  $\eta \cdot 28\text{GPa} \approx 25\text{GPa}$ . Since more critical defects could also be present in such a cable, this can be considered a statistically plausible upper bound for its strength, thus much lower than the ideal strength of nanotubes, today erroneously assumed in the megacable design (see Pugno 2006 and the related news at Nature, 22 May 2006: The space elevator: going down? by J. Palmer).

**Acknowledgements** The author thanks Prof. A. Capinteri for his kind invitation to intervene in a key-note lecture on this subject at the International Conference on Fracture XI.

## References

- Belytschko T (2004) The role of vacancy defects and holes in the fracture of carbon nanotubes. *Chem Phys Lett* 390: 413–420
- Belytschko T, Xiao SP, Ruoff R, (2002) Effects of defects on strength of nanotubes: experimental-computational comparison. Los Alamos National Laboratory, Preprint Archive, Physics pp 1–6
- Carpinteri A, Pugno N (2005) Are the scaling laws on strength of solids related to mechanics or to geometry? *Nat Mat* 4: 421–423.
- Freund LB (1990) *Dynamic fracture mechanics*. Cambridge University Press
- Gao H, Ji B, Jaeger IL, Arzt E, Fratzl P (2003) Materials become insensitive to flaws at nanoscale: lesson from nature. *Proc Natl Acad Sci USA* 100: 5597–5600
- Griffith AA (1920) The phenomenon of rupture and flow in solids. *Phil Trans Roy Soc A221*: 163–198
- Heizler SI, Kessler DA (2002) Mode-I fracture in a non-linear lattice with viscoelastic forces. *Phys Rev E* 66: 016126–1/10.
- Hellan K (1985) *An Introduction to fracture mechanics*. McGraw-Hill Book Company
- Hirai Y et al (2003) Molecular dynamics studies on mechanical properties of carbon nano tubes with pinhole defects. *Jpn J Appl Phys* 42: 4120–4123
- Holland D, Marder M (1999) Cracks and atoms. *Adv Mat* 11: 793–806
- Irwin GR (1957) Analysis of stresses and strains near the end of a crack traversing a plate. *Trans ASME J Appl Mech* E24: 361–364
- Kessler D, Levine H (2003) Does the continuum theory of dynamic fracture work? *Phys Rev E* 68:036118–1/4
- Marder M (1991) New dynamical equations for cracks. *Phys Rev Lett* 66: 2484–2487
- Marder M, Gross S (1995) Origin of crack tip instabilities. *J Mech Phys Sol* 43: 1–48
- Marder M, Liu X (1993) Instability in lattice fracture. *Phys Rev Lett* 71: 2417–2420
- Mielke SL, Troya D, Zhang S, Li J-L, Xiao S, Car R, Ruoff RS, Schatz GC,
- Mott NF, (1948) Brittle fracture in mild steel plates. *Engineering* 165: 16–18
- Morozov NF, Petrov Yu V, Utkin AA (1990) *Dokl Akad Nauk SSSR* 313(2): 276 [Sov Phys Dokl 35:646]
- Murakami H. (1986) *Stress intensity factors handbook*. Publ. Pergamon, Oxford, UK
- Neuber H (1958) *Theory of notch stresses*. Springer, Berlin
- Novozhilov V (1969) On a necessary and sufficient criterion for brittle strength. *Prikl Mat Mek*, 33: 212–222
- Ogata S, Shibutani Y (2003) Ideal tensile strength and band gap of single-walled carbon nanotube. *Phys Rev B* 68: 165409–1/4
- Orowan E (1948) Fracture and strength of solids. *Rep Progress Phys* XII: 185
- Owen DM, Zhuang SZ, Rosakis AJ, Ravichandran G (1998) Experimental determination of dynamic crack initiation and propagation fracture toughness in thin aluminum sheets. *Int J Fract* 90: 153–174
- Pechevnik L, Levine H, Kessler D, (2002) Steady-state mode I cracks in a viscoelastic triangular lattice. *J Mech Phys Sol* 50: 583–613
- Petrov Yu V, Sitnikova WV (2004) Dynamic cracking resistance of structural materials predicted from impact fracture on aircraft alloy. *Tech Phys* 49: 57–60
- Petrov Yu V (1996) Quantum analogy in the mechanics of fracture solids. *Phys Solid State* 38: 1846–1850
- Pugno N, Ruoff R (2004) Quantized fracture mechanics. *Phil Mag* 84(27): 2829–2845
- Pugno N (2006) On the strength of the nanotube-based space elevator cable: from nanomechanics to megamechanics. *J Phys-Condens Mat* 18: S1971–S1990
- Slepyan L (1981) Dynamics of brittle fracture in lattice. *Doklady Soviet Phys* 26: 538–540
- Tada H, Paris PC, Irwin GR (1985) *The stress intensity factor handbook* 2nd edn. Paris Productions Incorporated
- Taylor D, Cornetti P, Pugno N (2005) The fracture mechanics of finite crack extensions. *Eng Frac Mech* 72: 1021–1028
- Westergaard HM (1939) Bearing pressures and cracks. *J Appl Mech* 6: 49–53
- Yu M-F, Lourie O, Dyer MJ, Moloni K, Kelly TF, Ruoff, RS (2000) Strength and breaking mechanism of multiwalled carbon nanotubes under tensile load. *Science* 287: 637–640
- Zhang S, Mielke SL, Khare R, Troya D, Ruoff RS, Schatz GC, Belytschko T (2004) Mechanics of defects in carbon nanotubes: atomistic and multiscale simulations. *Phys Rev B* 71: 115403-1/12